

# A circular compact ultra-wideband antenna for 5G microwave applications

Swati Varun Yadav<sup>1</sup>, Manish Varun Yadav<sup>2</sup>, Tanweer Ali<sup>3</sup>, Sounik Kiran Kumar Dash<sup>4</sup>, Navya Thirumaleshwar Hegde<sup>2</sup>, Vishnu G. Nair<sup>2</sup>

<sup>1</sup>Department of Instrumentation and Control Engineering, Manipal Institute of Technology, Manipal Academy of Higher Education, Manipal 576104, India

<sup>2</sup>Department of aeronautical and Automobile Engineering, Manipal Institute of Technology, Manipal Academy of Higher Education, Manipal 576104, India

<sup>3</sup>Department of Electronics and Communication Engineering, Manipal Institute of Technology, Manipal Academy of Higher Education, Manipal 576104, India

<sup>4</sup>Department of Electronics and Communication Engineering, SRM Institute of Science and Technology, Kattankulathur, Tamil Nadu, 603203, India

## Article Info

### Article history:

Received Nov 9, 2023

Revised Feb 27, 2024

Accepted Mar 10, 2024

### Keywords:

5G

Current distribution

Gain

Slots

Ultra-wideband

## ABSTRACT

This article introduces an innovative circular and compact ultra-wideband (UWB) radiator designed specifically for 5G microwave applications. This antenna incorporates a “TU”-shaped ground plane on its reverse side, with strip lines feeding the circular element on the front side. Notably, the antenna exhibits impressive characteristics, including an outstanding impedance bandwidth of 107%, and an impressive return loss of -32 dB. Its operational frequency range spans from 2.4 GHz to 11 GHz, centered at 6.7 GHz. Extensive simulations were conducted using CST microwave studio software to validate its performance. The antenna’s physical dimensions are defined by a size of  $0.12 \lambda \times 0.08 \lambda \times 0.012 \lambda$  relative to its wavelength. Furthermore, this antenna demonstrates exceptional stability in its polar patterns and maintains a high-efficiency level, achieving a substantial gain of 3.75 dBi with an efficiency rating of 84.5%. These remarkable attributes make this antenna suitable for a wide range of applications, including Wi-Fi, 5G, WLAN, and various other microwave communication scenarios.

*This is an open access article under the [CC BY-SA](#) license.*



## Corresponding Author:

Tanweer Ali

Department of Electronics and Communication Engineering, Manipal Institute of Technology

Manipal Academy of Higher Education

Manipal 576104, India

Email: tanweer.ali@manipal.edu

## 1. INTRODUCTION

The high-frequency ultra-wideband (UWB) band radiator is a cutting-edge solution for multiple communication applications. This advanced antenna operates in the UWB band, which encompasses a high-frequency range, enabling seamless communication across various wireless technologies. The UWB band radiator boasts exceptional performance, offering superior data transfer rates, reduced latency, and enhanced capacity. With its innovative design and precise engineering, this radiator supports multiple communication protocols, making it ideal for next-generation wireless systems. Experience the power of high-frequency communication with the high-frequency UWB band radiator, an indispensable choice for diverse communication needs, from 5G and beyond. Embrace the future of wireless connectivity with this state-of-the-art radiator. Wireless communication extensively employs a compact size of antennas, each distinguished by its unique shapes and attributes. These antennas encompass a variety of designs such as semi-circular, L-shaped,

triangular, multi-slot, and U-shaped, among others, as documented in various sources [1]-[7]. To enhance the capabilities of these antennas, researchers have explored numerous techniques aimed at boosting their performance.

One notable strategy involves manipulating the antenna's ground plane by incorporating parasitic elements. This additional integration of elements has proven to significantly enhance antenna performance. Another avenue of exploration involves integrating small fractal components, which contribute to the overall improvement of antenna attributes. Circular and U-shaped slots have also been integrated into designs, affecting parameters like bandwidth and radiation patterns. The alteration of the circular patch's shape has been recognized as a means to achieve specific polar radiation patterns of interest [8]-[15]. Past research efforts have significantly advanced the capabilities of aerospace communication systems by extending their operational range. These advancements were made possible through innovative adaptations to antenna designs. For example, a pivotal breakthrough emerged when adjustments were introduced to a patch antenna known for its defective backside and incorporation of semi-circular slots [16]-[18]. Through careful modifications to these specific aspects of the antenna's structure, researchers successfully achieved a broadened bandwidth that aligns with the demands of aerospace communication. Furthermore, manipulating the antenna's backside by introducing modified slots has yielded intriguing results. This approach led to creation a patch element intentionally designed with a compromised plane, an unexpected characteristic that, counterintuitively, enhances the antenna's performance in certain contexts [19], [20]. These findings underscore the intricate nature of antenna design, where unconventional alterations can lead to unforeseen advantages. Beyond these pivotal discoveries, studies have delved into alternative alternatives to antenna designs aimed at enhancing performance. One notable exploration avenue involves using a flexible antenna alongside a radiator shaped in a "dumbbell" configuration [21], [22]. This innovative design highlights the diversity of creative solutions and underscores how unconventional geometries can contribute to desired outcomes in aerospace communication. Another proposed enhancement revolves around a long strip patch antenna strategically integrating rear-cut slots [23]. This design adaptation was conceived to optimize the flow of current within the antenna, ultimately resulting in improved performance characteristics. Such inventive design adjustments exemplify the iterative and forward-looking nature inherent to antenna engineering.

Ensuring balanced radiation patterns holds immense significance within the realm of antenna design. The achievement of equilibrium in radiation patterns guarantees uniform emission of signals across various directions, a fundamental prerequisite for effective communication. A noteworthy approach proposed to confront this challenge revolves around a deliberate adjustment to the antenna's rear side. This involves the strategic introduction of meticulously trimmed circular holes [24], [25]. This meticulous modification aims to exert control over signal propagation dynamics, culminating in a more consistent radiation pattern and elevated antenna performance.

Addressing the challenge of impedance matching, which is crucial for efficient power transfer between the antenna and transmission line, has led to integrating multi-slots within the antenna's structure [26]. Similarly, adopting the L-shaped design has proven instrumental in alleviating band resonance issues, thereby enhancing the antenna's proficiency within a desired frequency spectrum [27]. To expand the operational bandwidth, certain studies have explored the truncation of the antenna's ground plane [28]. This technique brings about alterations in signal propagation characteristics, empowering the antenna to cover a broader range of frequencies. In addition, researchers have directed their focus toward modifying the primary patch of the antenna to achieve heightened gain [29]. This adjustment entails reshaping the core element to optimize signal concentration and radiation efficiency, significantly contributing to overall performance enhancements.

## 2. GEOMETRY AND DESIGN STRUCTURE

Figures 1(a)-(e) illustrates the antenna's geometry and design concept. The physical dimensions of the exhibited antenna structure measure 11 mm in width, 15 mm in length, and 1.6 mm in thickness. This antenna design is implemented on an FR4 substrate and consists of annealed copper. The key dimensions of the antenna include "S2" for width and "S1" for length, as depicted in Figure 2. The substrate thickness, denoted as "H1," is associated with a microstrip line characterized by a length "S4" and width "S5." The patch design follows a straightforward circular configuration with a diameter "S3". Notably, the ground plane incorporates two symmetrical circular rings with a "R6" diameter, which contribute to improved performance at higher frequencies. Additionally, a "T"-shaped element is integrated vertically with dimensions "R10" for length and "R2" for width. Furthermore, the "U" section and horizontal segment are divided into three parts: flange, width, and length, with two symmetrical side rectangles. The flange is a rectangle with "R1" width and "R4" length within the antenna's backplane. To enhance performance, slots are introduced in the backplane structure. As designed, the antenna's ideal dimensions are 15mm in width, 11mm in length, and 1.6 mm in thickness. These structures are carved out of an FR4 substrate with a loss tangent and dielectric constant of 4.3. The top layer of the FR4 substrate is composed of annealed copper with a conductivity of  $5.8 \times 10^7$  S/m. The

design evolution of the proposed antenna is visually depicted in Figure 3, illustrating the gradual development of a circular, compact UWB radiator for 5G microwave applications.

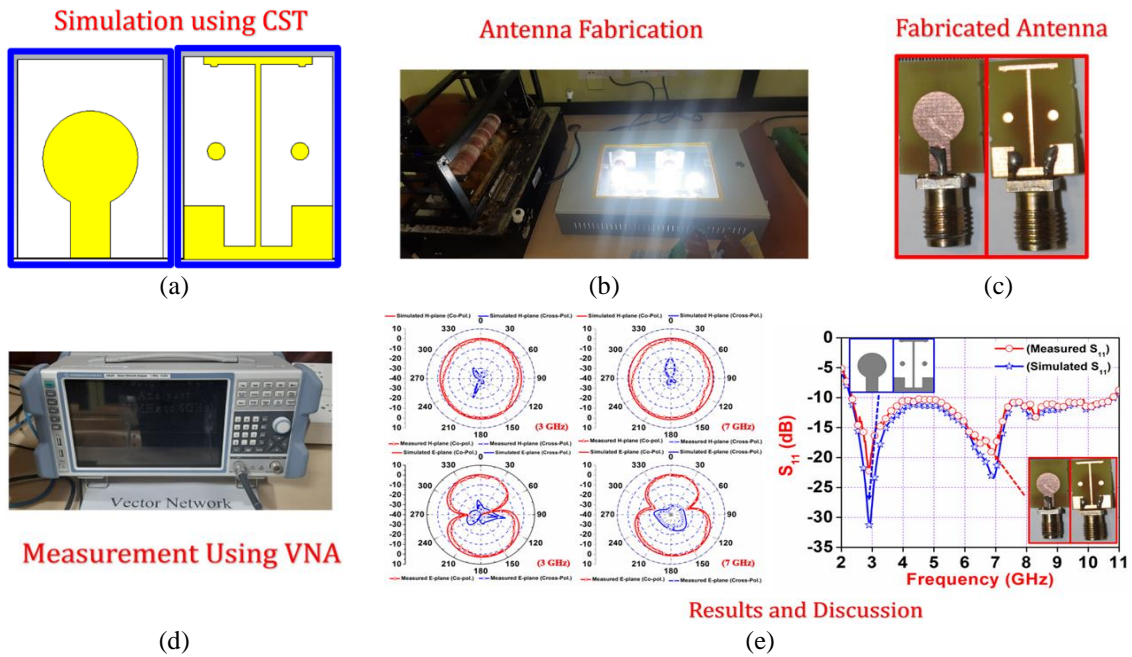


Figure 1. Graphical abstract for proposed approach: (a) simulated antenna using CST, (b) shows the fabrication unit available in the antenna laboratory, (c) fabricated antenna design, (d) testing and measurement, and (e) comparison of simulated and measured results

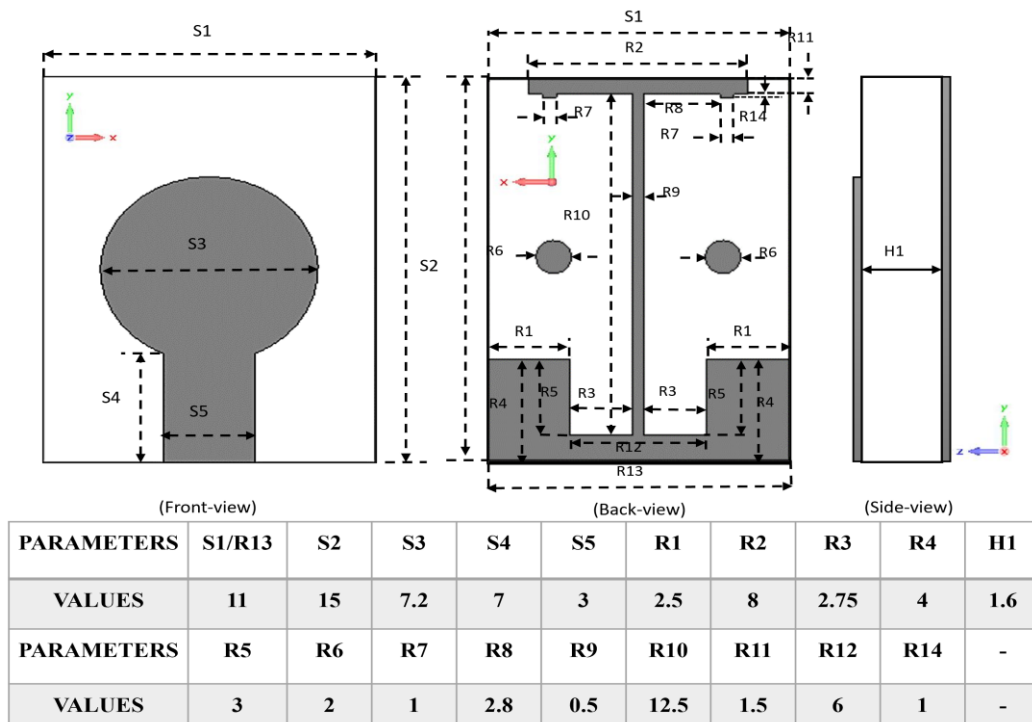


Figure 2. Geometry and conceptual design of an antenna

This progression is divided into four distinct phases: in step 1, the process commences by creating a basic circular patch with a full ground plane radiator. Step 2 enhances the design by introducing a half cut into rear side with two circular and one rectangular strip in the middle. Step 3 involves the etching of rectangular slot and lower down the ground plane. Step 4 marks the culmination of the antenna's construction by incorporating rectangular strip at the top of the ground plane, resulting in the finished product. Figure 3 provides an informative visualization of the antenna's evolution by displaying the proposed radiator's reflection coefficient ( $S_{11}$  magnitude). This figure provides an insightful overview of the antenna design's progression through various developmental stages.

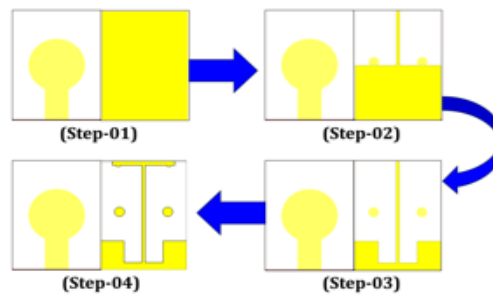


Figure 3. Evolution of the antenna

Step 01's initial configuration is characterized by a simple circular patch positioned above a stable ground plane, connected via a  $3 \text{ mm} \times 7 \text{ mm}$  microstrip line. The circular element has a diameter of 7.2 mm, and this setup results in a single-band resonance spanning from 3.8 to 9.5 GHz, as prominently depicted in Figure 4 moving forward to step 02, a significant transformation occurs on the antenna's rear side. Step 2 introduces a half-cut with two circular and one rectangular strip in the middle. This alteration leads to the emergence of dual-band resonances, covering frequencies from 3.4 to 5 GHz and 6 to 8.6 GHz, as clearly illustrated in Figure 4 step 3 involves further enhancements, including etching a rectangular slot and adjustments to the ground plane. These refinements improve impedance matching across lower-order and higher bands, effectively extending the antenna's frequency range from 3.2 to 8.5 GHz, as evidenced in Figure 4 in the final step, step 04, the antenna's construction is completed by incorporating a rectangular strip at the top of the ground plane. This last modification plays a crucial role in shifting the antenna's frequency range to a broader span, covering frequencies from 2.4 to 11 GHz, thereby concluding the comprehensive design process.

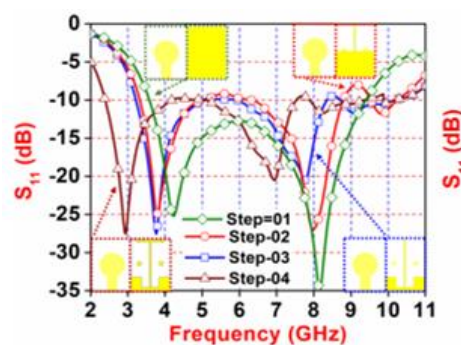


Figure 4. All stages  $S_{11}$  parameter

### 3. SIMULATED PARAMETER STUDY

In Figure 5, we delve into a comprehensive analysis of the frequency versus magnitude relationship of the return loss parameter,  $S_{11}$ , while manipulating the parameter "S3". The figure portrays a fascinating exploration of various frequency bands behavior as "S3" undergoes alterations. Specifically, we observe notable variations within the 2.4 to 8 GHz frequency range as "S3" is modified. This indicates that by adjusting "S3" we can influence and fine-tune the antenna's performance across different frequency bands.

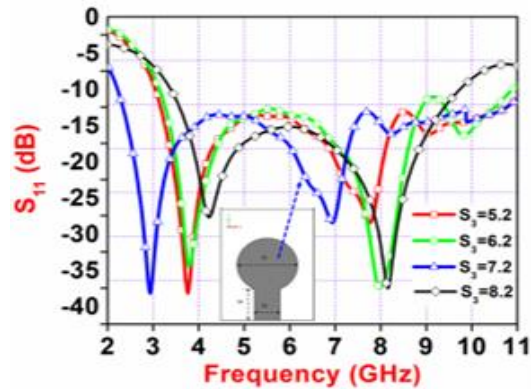


Figure 5. Simulated parameter sweep “Rc”

Furthermore, as we increase the value of “k” we notice even more pronounced variations, showcasing the sensitivity of the antenna’s behavior to this parameter. Similarly, when we enhance “S3” we achieve better performance in terms of frequency response. This insight highlights the importance of these parameter adjustments in optimizing the antenna’s characteristics.

Another critical parameter we scrutinized was the diameter of the circular element on the antenna’s backside, referred to as “S5”. Our investigation encompassed a range of sizes, from 2.5 mm to 3.5 mm, and it became evident that a diameter of 3 mm yielded the most favorable outcomes. This specific size was instrumental in achieving a balance between lower and higher-order resonances, a crucial aspect in antenna design. Moreover, it consistently maintained the magnitude of  $S_{11}$ , a key indicator of antenna performance, below -10 dB across a wide frequency spectrum spanning from 2.4 to 11 GHz. Figure 6 effectively visualizes how this adjustment in “S5” positively influenced the antenna’s performance, underscoring its significance in attaining a versatile and high-performing antenna design.

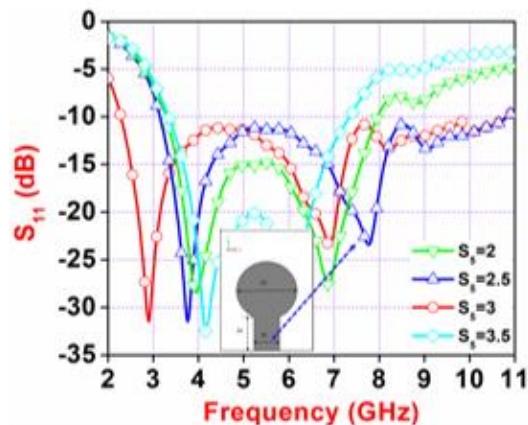


Figure 6. Simulated parameter sweep “Ry”

#### 4. MEASUREMENT AND SIMULATED RESULTS

In Figure 7, shows a visual representation of the relationship between frequency and input impedance, offering valuable insights into the antenna’s electrical characteristics. The graph shows that the behavior is primarily inductive within the 2–2.8 GHz frequency range, as indicated by a positive polarity in the curve. This suggests that at these frequencies, the antenna exhibits characteristics associated with inductance, where the impedance tends to resist changes in current. However, as the frequency increases beyond this range, there is a transition to a capacitive behavior, marked by a negative polarity in the curve. In this capacitive regime, the antenna’s impedance begins to favor the storage and release of electrical energy. It’s important to note that the impedance values are normalized to  $50 \Omega$ , providing a standardized reference point for evaluating the antenna’s performance across this frequency spectrum.

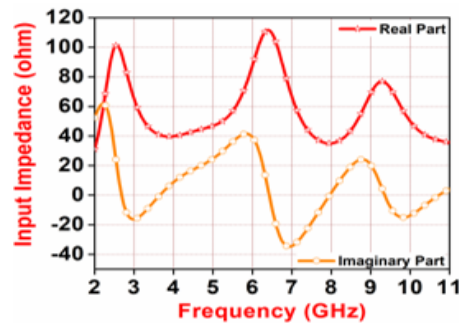


Figure 7. I/P impedance curve

Comprehensive measurements were conducted in an anechoic chamber to evaluate the proposed fabricated antenna's performance. The anechoic chamber provides an isolated and controlled testing environment, minimizing external reflections and interference. A vector network analyzer (VNA) was employed to measure key parameters, such as return loss, radiation patterns, and impedance characteristics. During the measurement process, the antenna was precisely positioned and oriented as per the experimental setup. Various measurements were performed with the antenna placed at different angles and orientations to capture its radiation patterns and evaluate its directional characteristics.

The proposed structure has undergone a comprehensive analysis to optimize its impact on the  $S_{11}$  parameter and other simulated outcomes. The measurement results were compared with theoretical simulations to validate the antenna's design and verify its performance, as illustrated in Figure 8. Deviations or discrepancies between the measurements and simulations were carefully analyzed to identify potential factors influencing the antenna's behavior. The proposed radiator demonstrates a wide impedance bandwidth, indicating its ability to operate effectively across a range of frequencies. The bandwidth is calculated as 107%, covering the frequency range from 2.4 GHz to 14 GHz. This broad impedance bandwidth is crucial for accommodating multiple communication bands and ensuring efficient signal transmission. A comparison between the simulated and measured return loss validates the accuracy of the simulation model, with close agreement observed. Minor discrepancies can be attributed to fabrication tolerances and measurement uncertainties. Nonetheless, the antenna demonstrates excellent impedance matching and performs admirably within the desired frequency band.

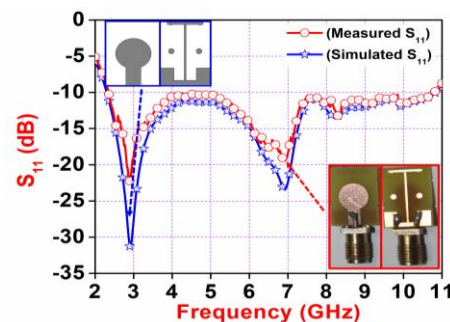


Figure 8. Return loss curve

Figure 9 is an illuminating visual representation, effectively showcasing the co-polarization and co-polarization patterns across distinct frequencies, specifically 6 GHz and 9 GHz. This depiction of the radiation pattern unfolds within the context of two orthogonal planes, affording a comprehensive insight into the antenna's behavior. More precisely, the "E" Plane occupies a position of  $90^\circ$  within the YoZ plane, while the "H" plane assumes a placement of  $0^\circ$  within the XoZ plane. The most salient characteristic evident within these radiation patterns is their notable stability and uniformity. This quality stands as a testament to the antenna's pronounced efficiency. By offering the visualization of radiation patterns within both orthogonal planes, a lucid understanding of the antenna's directional attributes at the specified frequencies is readily facilitated. The inclusion of both measured and simulated radiation patterns for the H- planes and E-planes in the illustration further enriches this comprehension. The unchanging nature of the radiation pattern across these

planes is of particular significance. This consistent behavior serves as a compelling indicator of the antenna’s well-behaved and harmonious performance. This unwavering nature essentially underscores that the antenna upholds a coherent functionality, thereby reinforcing its dependability and effectiveness in terms of both signal propagation and directional orientation.

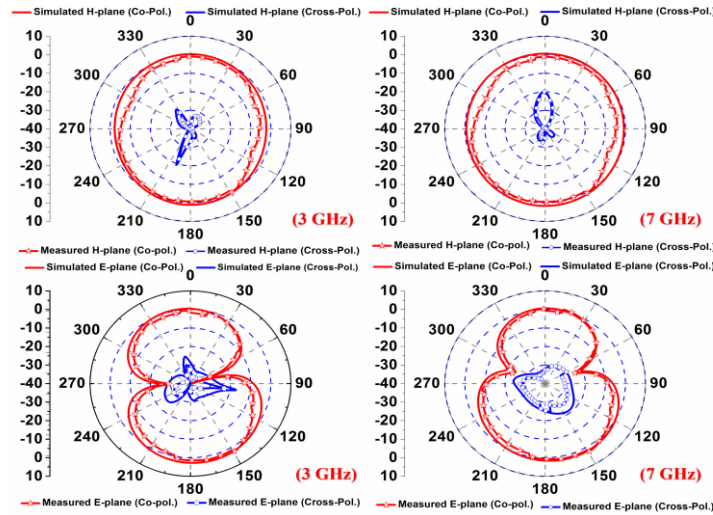


Figure 9. Co-polarization and cross-polarization radiation patterns

To visualize the antenna surface currents, we employed advanced electromagnetic simulation techniques. These simulations provide a detailed depiction of the current flow on the antenna’s conducting surfaces, allowing us to analyze their spatial distribution and intensity. Figure 10 showcases the simulated surface current distribution on the antenna. The colour contours represent the magnitude of the currents, with different colours indicating varying levels of current intensity. This visualization helps us identify areas of high current concentration and observe how the currents interact with different antenna elements. Studying the surface currents in the front and back view of the suggested antenna at 3 GHz frequency. Understanding the distribution and magnitude of surface currents aids in optimizing the antenna design and identifying any potential issues that could affect its performance.

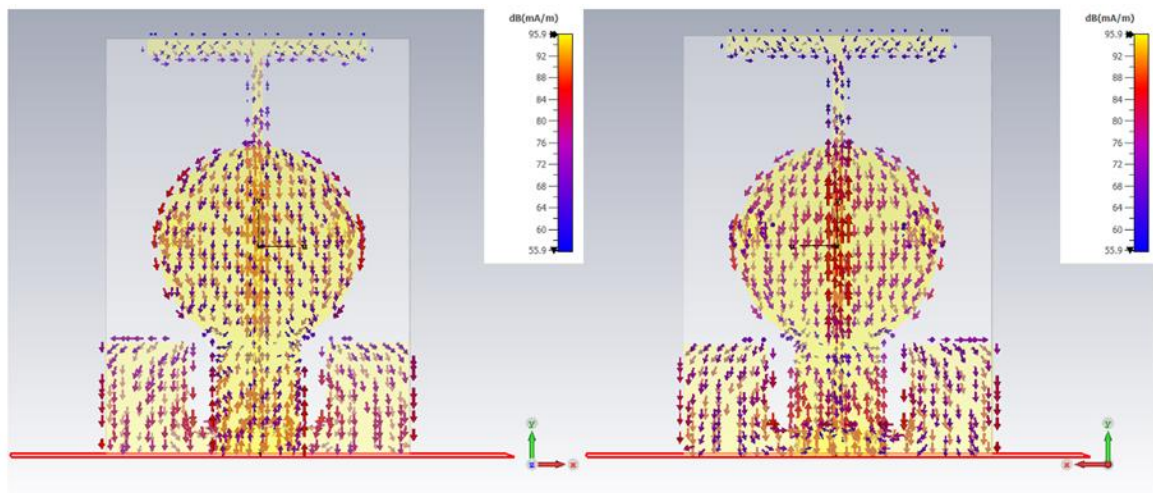


Figure 10. The current field distribution

In Figure 11, we observe the simulated radiation lobe pattern of the 5G antenna, with a specific focus on the 2D-vector surface current's frequency distribution at 3 GHz. This depiction encompasses both the front plane and back plane of the antenna structure. What's particularly noteworthy is the concept that by substituting the antenna with equivalent surface currents, the resulting radiated field closely mirrors the original antenna's surface current distribution. This intriguing phenomenon suggests that the surface current plays a pivotal role in facilitating radiation detection, even without the primary current source, emphasizing its significance in understanding and characterizing the antenna's radiation behaviour.

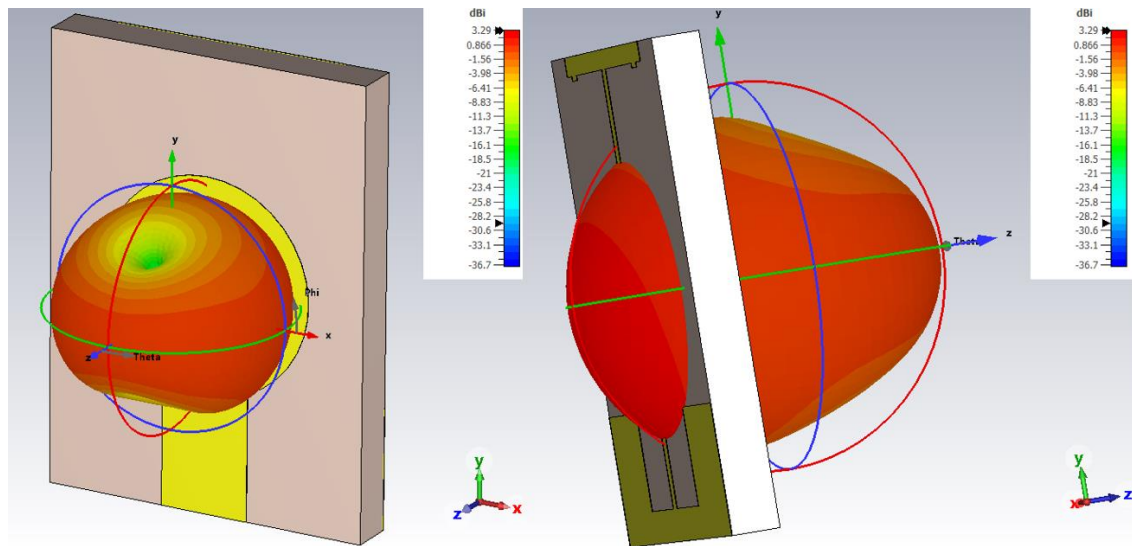


Figure 11. Simulated radiation lobe pattern

In Figure 12, we are presented with a revealing depiction of the antenna efficiency and gain simulation curve, offering valuable insights into the antenna's behavior across different frequencies. A conspicuous trend is the continuous increase in gain as the frequency rises. This signifies that the antenna becomes increasingly proficient at amplifying signals as we move toward higher frequencies. At the peak of this gain curve, which stands at an impressive 3.75 dB, we find the antenna's optimal performance occurring precisely at 7.2 GHz. At its zenith, the antenna radiation efficiency reaches an impressive value of 0.845, equivalent to an efficiency rate of 84.5%. This marks the frequency point of 5.5 GHz as the one where the antenna excels in radiating a substantial portion of the received signals, making it highly effective for communication purposes. Table 1 demonstrates a contrast between antennas that have been previously documented. After evaluating multiple parameters, it has been established through our analysis that the design we propose is smaller in dimensions and displays enhanced characteristics compared to the antennas previously documented.

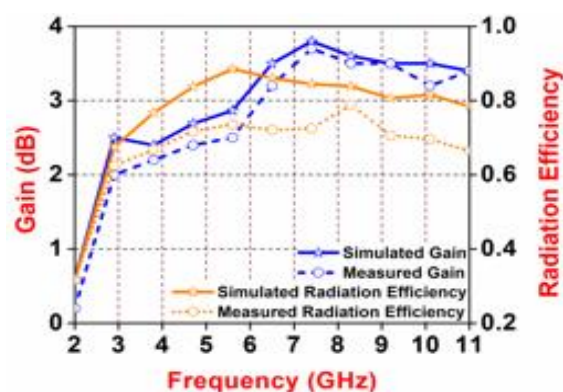


Figure 12. Simulated and measured gain and efficiency curve

Table 1. Comparison of published planar antennas

References	Band obtained (GHz)	Peak gain (dBi)	Fractional B/W (%)	Peak ( $\eta$ ) (%)	Overall volume (in $\lambda$ )
[2]	3.1–22	1.7	150	NA	$.28 \lambda \times .25 \lambda \times .016 \lambda$
[2]	3.1–11	5.1	110	89	$.20 \lambda \times .25 \lambda \times .015 \lambda$
[6]	3.9–14	3.5	142	75	$.26 \lambda \times .26 \lambda \times .019 \lambda$
[8]	2–9	4.5	127	62	$.33 \lambda \times .22 \lambda \times 0.1 \lambda$
[12]	3.5–19	3.2	145	81	$.23 \lambda \times .23 \lambda \times .015 \lambda$
[15]	3.1–11	2	109	60	$.55 \lambda \times .41 \lambda \times .022 \lambda$
[17]	2.9–16	5.2	139	87	$.33 \lambda \times .24 \lambda \times .014 \lambda$
[21]	2.8–12	2.79	122	72	$.18 \lambda \times .14 \lambda \times .15 \lambda$
[24]	2.7–7.3	2.3	108	78.3	$.32 \lambda \times .2 \lambda \times .014 \lambda$
[25]	3.1–11	2.2	110	69	$.14 \lambda \times .18 \lambda \times .015 \lambda$
[26]	2.3–11	2.1	129	70	$.2 \lambda \times .3 \lambda \times .014 \lambda$
Presented	2.4–11	3.7	107	84.5	$.12 \lambda \times .08 \lambda \times .012 \lambda$

## 5. CONCLUSION

This paper introduces a novel circular and compact UWB radiator designed for 5G microwave technology applications. Extensive analysis of simulation results reveals that this radiator, with dimensions measuring  $15 \times 11 \times 1.6 \text{ mm}^3$ , exhibits impressive performance characteristics. It achieves a peak gain of 3.75 dBi and boasts an efficiency rating of 84.5%. Furthermore, this antenna showcases a remarkably wide impedance bandwidth of 107%, centered around the 5.2 GHz frequency, spanning from 2.4 GHz to 11 GHz. The current distribution in the antenna demonstrates strong radiation capabilities. The design maintains a stable and consistent radiation pattern and offers a low-profile construction and excellent impedance matching. With its distinctive “TU” shape, this antenna is well-suited for diverse communication applications, including Wi-Fi, 5G, WLAN, and various other microwave communication scenarios.

## REFERENCES

- [1] B. Mishra, R. K. Verma, N. Yashwanth, and R. K. Singh, “A review on microstrip patch antenna parameters of different geometry and bandwidth enhancement techniques,” *International Journal of Microwave and Wireless Technologies*, vol. 14, no. 5, pp. 652–673, Jun. 2022, doi: 10.1017/S1759078721001148.
- [2] R. Przesmycki, M. Bugaj, and L. Nowosielski, “Broadband Microstrip Antenna for 5G Wireless Systems Operating at 28 GHz,” *Electronics*, vol. 10, no. 1, p. 1, Dec. 2020, doi: 10.3390/electronics10010001.
- [3] D. Imran *et al.*, “Millimeter wave microstrip patch antenna for 5G mobile communication,” in *2018 International Conference on Engineering and Emerging Technologies (ICEET)*, IEEE, Feb. 2018, pp. 1–6, doi: 10.1109/ICEET1.2018.8338623.
- [4] A. Khidre, K.-F. Lee, A. Z. Elsherbeni, and F. Yang, “Wide Band Dual-Beam U-Slot Microstrip Antenna,” *IEEE Transactions on Antennas and Propagation*, vol. 61, no. 3, pp. 1415–1418, Mar. 2013, doi: 10.1109/TAP.2012.2228617.
- [5] T. Kiran, N. Mounisha, C. Mythily, D. Akhil, and T. V. B. P. Kumar, “Design of Microstrip Patch Antenna for 5g Applications,” *IOSR Journal of Electronics and Communication Engineering (IOSR-JECE)*, vol. 13, no. 1, pp. 14–17, 2018.
- [6] J. Colaco and R. Lohani, “Design and Implementation of Microstrip Patch Antenna for 5G applications,” in *2020 5th International Conference on Communication and Electronics Systems (ICCES)*, IEEE, Jun. 2020, pp. 682–685, doi: 10.1109/ICCES48766.2020.9137921.
- [7] A. C. Shagar and S. D. Wahidabanu, “Novel wideband slot antenna having notch-band function for 2.4 GHz WLAN and UWB applications,” *International Journal of Microwave and Wireless Technologies*, vol. 3, no. 4, pp. 451–458, 2011, doi: 10.1017/S1759078711000183.
- [8] S. Baudha, K. Kapoor, and M. V. Yadav, “U-Shaped Microstrip Patch Antenna with Partial Ground Plane for Mobile Satellite Services (MSS),” in *2019 URSI Asia-Pacific Radio Science Conference (AP-RASC)*, IEEE, Mar. 2019, pp. 1–5, doi: 10.23919/URSIAP-RASC.2019.8738196.
- [9] A. Kurniawan and S. Mukhlisin, “Wideband Antenna Design and Fabrication for Modern Wireless Communications Systems,” *Procedia Technology*, vol. 11, pp. 348–353, 2013, doi: 10.1016/j.protcy.2013.12.201.
- [10] A. Ghosh, S. K. Ghosh, D. Ghosh, and S. Chattopadhyay, “Improved polarization purity for circular microstrip antenna with defected patch surface,” *International Journal of Microwave and Wireless Technologies*, vol. 8, no. 1, pp. 89–94, Feb. 2016, doi: 10.1017/S1759078714001305.
- [11] S. Verma, L. Mahajan, R. Kumar, H. S. Saini, and N. Kumar, “A small microstrip patch antenna for future 5G applications,” in *2016 5th International Conference on Reliability, Infocom Technologies and Optimization (Trends and Future Directions) (ICRITO)*, IEEE, Sep. 2016, pp. 460–463, doi: 10.1109/ICRITO.2016.7784999.
- [12] A. M. Abdelraheem and M. A. Abdalla, “Compact curved half circular disc-monopole UWB antenna,” *International Journal of Microwave and Wireless Technologies*, vol. 8, no. 2, pp. 283–290, Mar. 2016, doi: 10.1017/S1759078714001524.
- [13] S. Baudha, S. Gupta, and M. V. Yadav, “Parasitic rectangular patch antenna with variable shape ground plane for satellite and defence communication,” in *2019 URSI Asia-Pacific Radio Science Conference, AP-RASC 2019*, IEEE, Mar. 2019, pp. 1–4, doi: 10.23919/URSIAP-RASC.2019.8738654.
- [14] N. M. Awad and M. K. Abdelazeez, “Multislot microstrip antenna for ultra-wide band applications,” *Journal of King Saud University - Engineering Sciences*, vol. 30, no. 1, pp. 38–45, Jan. 2018, doi: 10.1016/j.jksues.2015.12.003.
- [15] W. An, Y. Li, H. Fu, J. Ma, W. Chen, and B. Feng, “Low-Profile and Wideband Microstrip Antenna With Stable Gain for 5G Wireless Applications,” *IEEE Antennas and Wireless Propagation Letters*, vol. 17, no. 4, pp. 621–624, Apr. 2018, doi: 10.1109/LAWP.2018.2806369.
- [16] R. Rashmitha, N. Niran, A. A. Jugale, and M. R. Ahmed, “Microstrip Patch Antenna Design for Fixed Mobile and Satellite 5G Communications,” *Procedia Computer Science*, vol. 171, pp. 2073–2079, 2020, doi: 10.1016/j.procs.2020.04.223.

- [17] M. G. Tampouratzis, E. Katsos, D. Vouyioukas, D. Stratakis, and T. Yioultis, "Design of Planar CPW-Fed UWB Trapezoidal Monopole Antennas with Band Rejection Characteristics," in *2022 26th International Conference on Circuits, Systems, Communications and Computers (CSCC)*, IEEE, Jul. 2022, pp. 250–255, doi: 10.1109/CSCC55931.2022.00049.
- [18] S. Hota, M. Varun Yadav, S. Baudha, and B. B. Mangaraj, "Miniaturized planar ultra-wideband patch antenna with semi-circular slot partial ground plane," in *2019 IEEE Indian Conference on Antennas and Propagation (InCAP)*, IEEE, Dec. 2019, pp. 1–4, doi: 10.1109/InCAP47789.2019.9134577.
- [19] Sakshi and M. Bharti, "Penta-band Planar Monopole Circular Antenna Design Using Inverted L-Shaped Slot for UWB Application," *Journal of Electronic Materials*, vol. 52, no. 12, pp. 8281–8292, Dec. 2023, doi: 10.1007/s11664-023-10744-9.
- [20] I. Marasco *et al.*, "Design and Fabrication of a Plastic-Free Antenna on a Sustainable Chitosan Substrate," *IEEE Electron Device Letters*, vol. 44, no. 2, pp. 341–344, Feb. 2023, doi: 10.1109/LED.2022.3232986.
- [21] R. Lakshmanan and S. K. Sukumaran, "Flexible Ultra Wide Band Antenna for WBAN Applications," *Procedia Technology*, vol. 24, pp. 880–887, 2016, doi: 10.1016/j.protcy.2016.05.149.
- [22] J. Saini and S. K. Agarwal, "Design a single band microstrip patch antenna at 60 GHz millimeter wave for 5G application," in *2017 International Conference on Computer, Communications and Electronics (Comptelix)*, IEEE, Jul. 2017, pp. 227–230, doi: 10.1109/COMPTELIX.2017.8003969.
- [23] H. Xia *et al.*, "A Cost-Effective Wideband Dual-Polarized L-Shaped Probe-Fed Phased Array Antenna for 60-GHz AiP Applications," *IEEE Transactions on Components, Packaging and Manufacturing Technology*, vol. 13, no. 11, pp. 1790–1803, Nov. 2023, doi: 10.1109/TCPMT.2023.3319035.
- [24] A. A. Abdulbari *et al.*, "Design compact microstrip patch antenna with T-shaped 5G application," *Bulletin of Electrical Engineering and Informatics*, vol. 10, no. 4, pp. 2072–2078, Aug. 2021, doi: 10.11591/eei.v10i4.2935.
- [25] Y. Jandi, F. Gharnati, and A. Oulad Said, "Design of a compact dual bands patch antenna for 5G applications," in *2017 International Conference on Wireless Technologies, Embedded and Intelligent Systems (WITS)*, IEEE, Apr. 2017, pp. 1–4, doi: 10.1109/WITS.2017.7934628.
- [26] S. M. Mazinani and H. R. Hassani, "A Novel Broadband Plate-Loaded Planar Monopole Antenna," *IEEE Antennas and Wireless Propagation Letters*, vol. 8, pp. 1123–1126, 2009, doi: 10.1109/LAWP.2009.2033952.
- [27] M. V. Yadav, S. Baudha, and S. Thukral, "A Compact Hammer Shaped Printed Antenna With Parasitic Elements For Defense And Mobile Satellite Applications," in *2021 IEEE Indian Conference on Antennas and Propagation (InCAP)*, IEEE, Dec. 2021, pp. 521–524, doi: 10.1109/InCAP52216.2021.9726331.
- [28] S. Baudha, M. V. Yadav, and Y. Bansal, "A COMPACT SLOT ANTENNA FOR ULTRA-WIDEBAND APPLICATIONS," *Telecommunications and Radio Engineering*, vol. 79, no. 3, pp. 213–222, 2020, doi: 10.1615/TelecomRadEng.v79.i3.30.
- [29] G.-H. Kim and T.-Y. Yun, "Compact Ultrawideband Monopole Antenna With an Inverted-L-Shaped Coupled Strip," *IEEE Antennas and Wireless Propagation Letters*, vol. 12, pp. 1291–1294, 2013, doi: 10.1109/LAWP.2013.2283863.

## BIOGRAPHIES OF AUTHORS



**Swati Varun Yadav**     is an Assistant Professor in the Department of Instrumentation and Control Engineering, Manipal Institute of Technology, Manipal Academy of Higher Education, Manipal, Karnataka. She received his B.E. degree in Electronics and Communication Engineering from MIT, College, Ujjain (India) in 2007 and received his M.E. degree in Digital Communication from Rajiv Gandhi Proudhyogiki Vishwavidyalaya, Bhopal (India) in 2011. Ph.D. degree from Department of Electrical and Electronics Engineering, Goa Campus, BITS, Pilani, (India) in 2023. Her fields of interest are high power microwave devices, mode converters, and planar antenna. She can be contacted at email: yadav.swati@manipal.edu.



**Manish Varun Yadav**     is an Assistant Professor in the Department of Aeronautical and Automobile Engineering, Manipal Institute of Technology, Manipal Academy of Higher Education, Manipal, Karnataka, he received his B.E. degree in Electronics and Communication Engineering from Government Engineering College, Ujjain (India) in 2007 and received his M.E. degree in Digital Communication from Rajiv Gandhi Proudhyogiki Vishwavidyalaya, Bhopal (India) in 2011. Ph.D. degree from Department of Electrical and Electronics Engineering, Goa Campus, BITS, Pilani, (India) in 2022. His fields of interest are microstrip antenna and planar antenna. He is a Life Member of the India Society of Technical Education (ISTE) and a Senior member of the Institute of Electrical and Electronics Engineers (IEEE, Member). He can be contacted at email: yadav.manish@manipal.edu.



**Tanweer Ali**    is currently an Associate Professor with the Department of Electronics and Communication Engineering, Manipal Institute of Technology, Manipal Academy of Higher Education, Manipal. He is an active researcher in the field of microstrip antennas, wireless communication, and microwave imaging. He has been listed in the top 2% scientists across the world for the years 2021 and 2022 by the prestigious list published by Stanford University, USA, indexed by Scopus. He has led seven Indian patents, of which three have been published. He is on the Board of a Reviewer of journals, such as the IEEE Transactions on Antennas and Propagation, IEEE Antennas and Wireless Propagation Letters, and IEEE Access. He can be contacted at email: tanweer.ali@manipal.edu.



**Sounik Kiran Kumar Dash**    received his Ph.D. from National Institute of Technology (NIT) Silchar, Assam, India in 2018. At present he is working as Research Assistant Professor in the Department of ECE, SRM Institute of Science and Technology (SRM IST), Chennai. Before joining SRM IST, he was working as a Research Scientist (A) at National University of Singapore (NUS) between 2022-2023, as a Postdoctoral Researcher at Southern University of Science and Technology, Shenzhen, China between 2019-21, as an Assistant Professor in the Department of ECE at CHRIST (Deemed to be University), Bengaluru, India between 2018-2019. His current research interests include substrate integrated waveguides, dielectric resonator antennas (dras), self-multiplexing antennas, rf energy harvesting, and MIMO antennas. He has authored or co-authored over forty research articles in referred journals published by IEEE, IET, and Wiley. And international conference proceedings (like URSI-GASS, EuMW, AEMC, and so on) of repute. He can be contacted at email: sounikkiran@gmail.com.



**Navya Thirumaleshwar Hegde**    has Master's degree in Astronomy and Space Engineering and Ph.D. in Aerospace System Modelling and Control from MIT, MAHE, Manipal. She is presently an Assistant professor in the Department of Aeronautical and Automobile Engineering, MIT, MAHE, Manipal. She has experience in system modelling, UAV, control system design, ADAS, autonomous vehicles. She can be contacted at email: navya.hegde@manipal.edu.



**Vishnu G. Nair**    received his Ph.D. degree from National Institute of Technology, Karnataka, India. He is presently an Associate Professor in the Department of Aeronautical and Automobile Engineering, Manipal Institute of Technology, Manipal Academy of Higher Education, Manipal. His research interest is in multi robotic systems, system modeling, autonomous vehicle and UAV. He can be contacted at email: vishnu.nair@manipal.edu.